Experimental Detection of a Majorana Mode in the core of a Magnetic Vortex inside a Topological Insulator-Superconductor $Bi_2Te_3/NbSe_2$ Heterostructure

Jin-Peng Xu,[1] Mei-Xiao Wang,[1] Zhi Long Liu,[1] Jian-Feng Ge,[1] Xiaojun Yang,[2] Canhua Liu,[1,5,*] Zhu An Xu,[2,5] Dandan Guan,[1] Chun Lei Gao,[1] Dong Qian,[1] Ying Liu,[1,3,5] Qiang-Hua Wang,[4,5] Fu-Chun Zhang,[2,5] Qi-Kun Xue,[6] and Jin-Feng Jia[1,5,†]

[1]*Key Laboratory of Artificial Structures and Quantum Control (Ministry of Education), Department of Physics and Astronomy, Shanghai Jiao Tong University, Shanghai 200240, China*

[2]*State Key Laboratory of Silicon Materials and Department of Physics, Zhejiang University, Hangzhou 310027, China*

[3]*Department of Physics, Pennsylvania State University, University Park, Pennsylvania 16802, USA*

[4]*National Laboratory of Solid State Microstructures and School of Physics, Nanjing University, Nanjing 210093, China*

[5]*Collaborative Innovation Center of Advanced Microstructures, Nanjing University, Nanjing 210093, China*

[6]*State Key Laboratory for Low-Dimensional Quantum Physics, Department of Physics, Tsinghua University, Beijing 100084, China*

(Received 29 August 2014; revised manuscript received 20 November 2014; published 7 January 2015)

Majorana fermions have been intensively studied in recent years for their importance to both fundamental science and potential applications in topological quantum computing. They are predicted to exist in a vortex core of superconducting topological insulators. However, it is extremely difficult to distinguish them experimentally from other quasiparticle states for the tiny energy difference between Majorana fermions and these states, which is beyond the energy resolution of most available techniques. Here, we circumvent the problem by systematically investigating the spatial profile of the Majorana mode and the bound quasiparticle states within a vortex in Bi_2Te_3 films grown on a superconductor $NbSe_2$. While the zero bias peak in local conductance splits right off the vortex center in conventional superconductors, it splits off at a finite distance $\sim$20 nm away from the vortex center in Bi_2Te_3. This unusual splitting behavior has never been observed before and could be possibly due to the Majorana fermion zero mode. While the Majorana mode is destroyed by the interaction between vortices, the zero bias peak splits as a conventional superconductor again. This work provides self-consistent evidences of Majorana fermions and also suggests a possible route to manipulating them.

DOI: 10.1103/PhysRevLett.114.017001 PACS numbers: 74.55.+v, 68.37.Ef, 74.25.Ha, 74.45.+c

Identical to their antiparticles, Majorana fermions (MF) were proposed in 1937 as an alternative to Dirac theory of ordinary fermions that carry opposite charge from their antiparticles [1]. Neutrinos are the first candidate for MF in particle physics, but their Majorana status remains to be confirmed [2]. There are also proposals that quasiparticles in certain quantum condensed matter systems may be MFs. Examples include 5/2 fractional quantum Hall state, cold atoms, and chiral p-wave superconductors [3,4]. Experimental realization of MFs is of great significance in fundamental physics. MFs obey non-Abelian statistics, and thus can be used to develop topological quantum computation. The recent work by Fu and Kane predicted that MFs should be present as zero-energy bound states at vortex cores of an engineered heterostructure consisting of a normal s-wave superconductor (SC) and a topological insulator (TI) [5]. Cooper pairs are introduced via the proximity effect to the TI surface where spin and momentum are locked in the topological surface state (TSS) band [6,7]. This leads to an unusual p-wave-like paired state that is time-reversal invariant and robust against disorder [8]. Theoretical studies later showed that the MFs may also reside at two ends of a semiconductor nanowire (NW) with strong spin-orbit coupling when it is contacted to an s-wave SC in a proper external magnetic field [9]. Several transport measurements revealed a signature of MFs, i.e., a sharp zero-bias peak in differential conductance spectrum, in various NW-SC junctions [10–14]. In InSb/Nb junction, an unconventional fractional ac Josephson effect was observed and attributed to the existence of MFs [15]. However, alternative explanations of these transport results based on disorder and/or band bending in the NWs have been proposed [16–19]. Very recently, S. Nadj-Perge *et al.* have reported their observation of MF on Fe atomic chains [20], as yet, no conclusive evidence has been established for the existence of MF [21].

In contrast, the disorder alone is unlikely to induce a zero-bias peak in a superconducting TI, which can be used to detect MFs without the complications mentioned above. Proximity effect induced superconductivity in a TI surface has been demonstrated in several TI/SC heterostructures [22–25]. To obtain the evidence for the existence of MFs, a promising route is to detect the zero-bias bound state at vortex cores of a TI/SC heterostructure with scanning

tunneling microscopy and spectroscope (STM/STS), so that a single Majorana mode at a vortex core can be explicitly identified.

Very recently, we have succeeded in constructing TI-SC heterostructures with an atomically smooth interface by growing epitaxial thin films of Bi_2Se_3 and Bi_2Te_3 on $NbSe_2$ single crystals, where coexistence of Cooper pairs and TSS was illustrated [26,27]. Abrikosov vortices and Andreev bound states therein were observed in the $Bi_2Te_3/NbSe_2$ heterostructure with STM and STS [27]. The major difficulty to distinguish the zero mode MF in the vortex core is the tiny energy gap separating it from the conventional quasiparticle states, i.e., the Caroli–de Gennes–Matricon states, [28–30]. The energy gap is estimated to be $0.83\Delta^2/\sqrt{\Delta^2 + E_D^2}$, where Δ is the superconducting gap and E_D is the Fermi energy relative to the Dirac point of the TSS band [31]. For $\Delta \sim 1$ meV and $E_D \sim 100$ meV, the minigap is ~0.01 meV, which is much smaller than the present energy resolution (0.1 meV) in STS. One way to increase the mini gap is to tune the Fermi level toward the Dirac point. However, in that case, the superconducting gap Δ becomes very small and the transition temperature becomes very low due to the weaker proximity effect; hence, the direct observation of the Majorana mode is still difficult. Fortunately, the Majorana mode is not pinned at the central point of a vortex core, but extensively distributes around the core center [32], which gives an opportunity to detect the MF by investigating the spatial distribution of the bound states in the vortex core. In this work, with STM and STS performed at 400 mK, we studied in detail the spatial distributions of the bound states in vortices of TI-SC heterostructures at different TI thickness. We reveal that the distinction between thick and thin TI films is very remarkable, which is attributed to the existence of MFs located at the vortex cores of thick TI samples.

Figure 1(a) is a schematic illustration for the configuration of the TI-SC heterostructure made by molecular beam epitaxy [33,34]. Bi_2Te_3 thin films were grown on $NbSe_2$ in a layer-by-layer mode, resulting in very large atomically smooth terraces on the Bi_2Te_3 surface suited for vortices measurement by STS (the details on sample preparation is in the Supplemental Material [35]). As we shall describe below, the carriers of the systems with 3 quintuple layers (QL) or less are almost from the bulk, and thus the vortex states are essentially the same as those in conventional s-wave superconductors. Systems with 5 or 6 QL are topological insulators and the vortex states are expected to host MFs. We have simulated a single vortex for 5 QL TI on top of a conventional s-wave SC. Our calculation shows that there is a pair of MFs, one at the surface and the other at the interface between the TI and the conventional SC, in the vortex core, as illustrated in Fig. 1(b). We show the probability density for the lowest-lying quasiparticle state in a view field $100 \times 100 \times 5$ of a

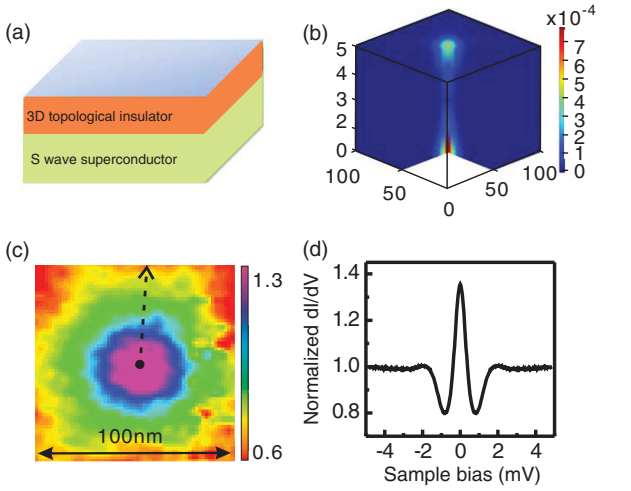

FIG. 1 (color). (a) A schematic illustration of topological insulator-superconductor heterostructure. (b) The calculated results showing two Majorana modes in a vortex core on 5 QL $Bi_2Te_3/NbSe_2$. (c) A vortex mapped by zero-bias dI/dV on 5 QL $Bi_2Te_3/NbSe_2$ at 0.1 T and 0.4 K. (d) A sharp zero-bias peak in the dI/dV spectrum measured at the center of the vortex in (c).

lattice model of the 5 QL TI. The amplitude is mainly concentrated on the top and bottom layers. The extent of the wave function is slightly larger on the top layer, as we assumed that the proximity induced pairing potential is about 50% smaller on the top layer than that on the bottom layer to cope with the experimental results (details for the numerics can be found in the Supplemental Material [35]). The probability distribution in Fig. 1(b) is in contrast to that in an otherwise conventional vortex line where it would be roughly uniform along the line instead (see Fig. S2 in the Supplemental Material[35]).

Figure 1(c) shows a typical contour of zero-bias differential conductance (ZBC) taken on a 5 QL Bi_2Te_3 film in an external magnetic field of 0.1 T. An Abrikosov vortex is clearly seen, which exhibits higher ZBC values due to the suppression of superconductivity within the vortex. Increasing the magnetic field would decrease the distance of the vortices that exhibit an ordered hexagonal lattice, as shown in Fig. S3. At the center of the vortex, a peak in dI/dV due to the bound quasiparticle states can be measured as shown in Fig. 1(d) (see the Supplemental Material [35] for the experimental conditions).

Along the dashed line directing to a nearest neighbor vortex, as indicated in Fig. 1(c) as well as in Fig. S3 [35], we measured the spatial variation of the dI/dV spectra as a function of distance (r) away from the vortex center. The results are given in Fig. 2(a). One can see that only one peak appears at zero bias in the dI/dV spectra near the vortex center, and the peak splits into two at a finite distance r. The splitting energy increases linearly with r. For a better view, we plot dI/dV as functions of r and sample bias V in a fake color image in Fig. 2(b), where the positions of the dI/dV peaks are indicated by red crosses. Two dotted lines are

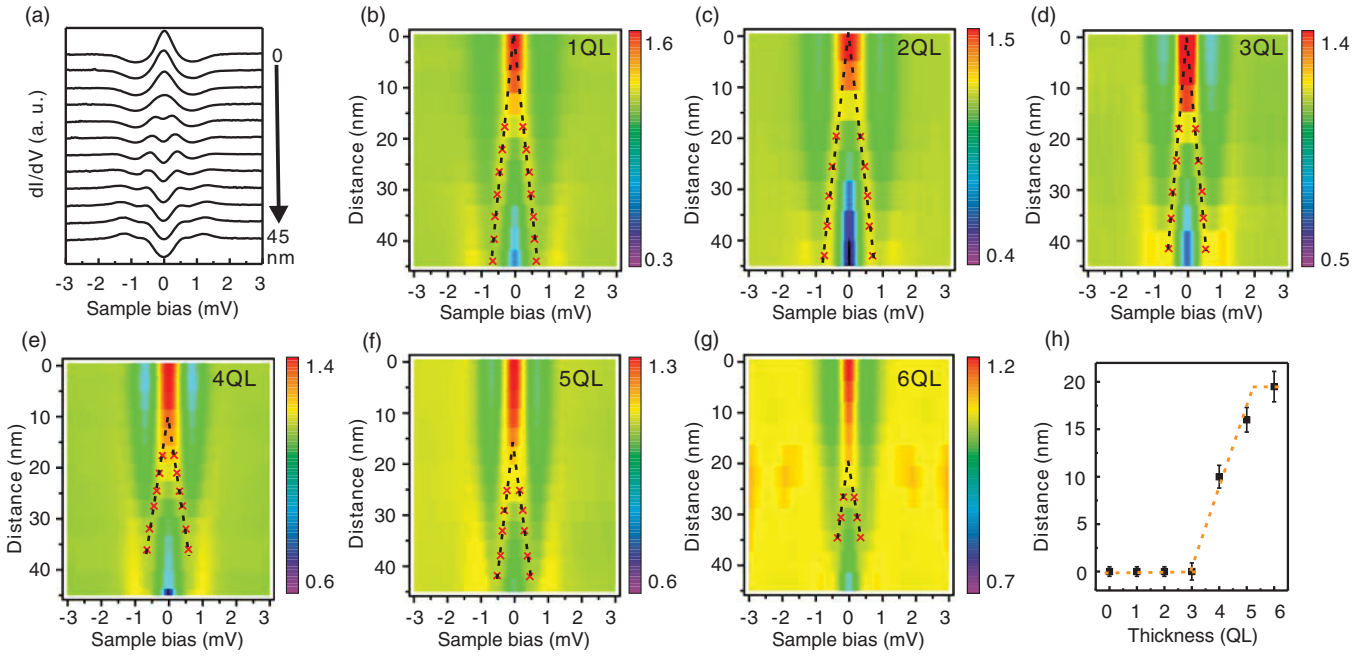

FIG. 2 (color). (a) A series of dI/dV curves measured along the black dashed line in Fig. 1(c), showing the peak of bound states splits into two at positions away from the vortex center. (b) The color image of (a) for a better view. The split peak positions in the dI/dV spectra are marked by red crosses, and the dotted lines superimposed on the crosses indicate the start point of the peak splitting. (c)–(g) The experimental results for 2–6 QL samples, following the similar data process of (b). (h) A summary of the start points of the peak split, showing a crossover at 4 QL.

drawn to illustrate the linear relation between the energy of the split peaks and the distance r. Extrapolate the lines, the cross point also gives out the splitting start point. The results for 2 to 6 QL Bi_2Te_3 films are shown in Figs. 2(c)–2(g). Although the splitting can be resolved almost at the same position ~20 nm from the center, the splitting start points (the cross points of the dotted lines) are obviously different for different films. For 1–3 QL Bi_2Te_3 films, the peak splits right off the vortex center (zero-distance splitting), similar to that in a conventional s-wave superconductor, such as $NbSe_2$ (Refs. [36,37]). In contrast, for the thicker Bi_2Te_3 films (4–6 QL), the splitting starts at a spatial point away from the vortex center (finite-distance splitting), an apparent deviation from that in a conventional superconductor. The peak splitting start position as a function of the thickness of Bi_2Te_3 films is summarized in Fig. 2(h); a transition at 4 QL can be clearly observed. It is noted that along another high symmetry direction that connects two next-nearest neighbor vortices, as indicated by the dotted line in Fig. S3, similar peak splitting behavior is also observed, as shown in Fig. S4.

The finite-distance splitting behavior of the bound states has not been reported before. We interpret this new feature related to the topological property of the local electronic structure. For the 4–6 QL, the Fermi level lies near the top of the Dirac bands, and also crosses the bottom of the bulk conduction bands (see Fig. 4). The local density of states (LDOS) of a vortex as measured in our STM is contributed to from both the bulk and the topological surface states. The bulk contribution is similar to that in a conventional superconductor, and the LDOS or the dI/dV spectra contributed from the bulk has a maximum (peak) at a final energy value proportional to the spatial distance r, see Fig. 2(b), for instance. In what follows we will argue that the MF mode of the 2D surface state may change the profile of the dI/dV spectra. For simplicity, we shall neglect the LDOS contribution from the quasiparticle bound states in two dimensions, since their contribution is expected to be similar to that from the bulk. The Majorana mode in the vortex core has been studied theoretically in Ref. [32]. They calculated the LDOS for the $Nb/Bi_2Se_3/Nb$ sandwich structure, and showed that the MF mode has a spatial distribution of about 40 nm, with a sharp peak at zero bias in the dI/dV spectrum near the vortex core. Our sample structure has similar parameters, so the spatial extension of the Majorana mode should be similar, although the envelope function depends on the Fermi wave vector. The Majorana mode is then expected to enhance the zero bias LDOS within a range of spatial distance $r \sim 40$ nm away from the vortex core, hence to possibly shift the maximum of the LDOS from a finite energy to zero bias energy for small r. The large zero bias LDOS at small r of the MF mode should be the underlying physics for the deviation of the zero distance splitting behavior of the bound state as we observed. Our STM measurement has an energy resolution of about 0.2 meV. The LDOS within this

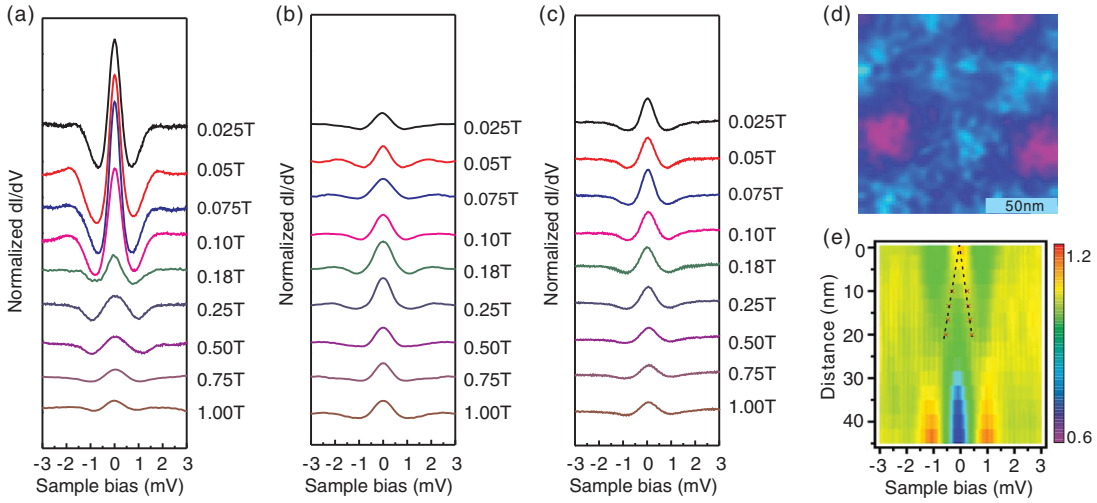

FIG. 3 (color). A series of dI/dV spectra measured at various magnetic fields at a vortex center of 5 QL $Bi_2Te_3/NbSe_2$ (a), bare $NbSe_2$, (b) and 2 QL $Bi_2Te_3/NbSe_2$ (c). A dramatic drop in the peak intensity is clearly seen at 0.18 T in (a). (d) Vortex lattice measured at 0.18 T on the 5 QL $Bi_2Te_3/NbSe_2$. The average distance between two adjacent vortices is about 110 nm. (e) The color image of dI/dV spectra measured at the vortex cores shown in (d). The crosses and dotted lines are the same indicators as those in Fig. 2(b). The peak-splitting start point is zero, in sharp contrast to that in Fig. 2(f).

energy resolution is expected to be enhanced due to the MF mode. We may argue that the maximum of LDOS for a fixed r may shift towards lower energy and the energy shift is less for larger r. These may explain the basic features in our observation of the finite-distance splitting. Note that the effect of the MF mode to the change of the LDOS in the vortex core depends on the relative weight of the MF mode. A systematic study of the LDOS of a vortex with both the bulk and Dirac surface states will require further study. In brief, we interpret the observation of a finite-distance split pattern as a demonstration of the MF in the center area of the vortex.

Our explanation is also supported by the magnetic field dependence of the LDOS of the 5 QL system. The dI/dV spectra taken at a vortex center of a 5 QL Bi_2Te_3 film in various magnetic fields are shown in Fig. 3(a). The zero-bias peak is very strong at a field less than 0.1 T. As the field reaches 0.18 T, the zero-bias peak becomes much weaker. In a conventional s-wave SC the vortex density is proportional to the magnetic field below a critical field H_{c2}. A single vortex structure is not sensitive to the external field and the LDOS near a vortex core is essentially unchanged as the field increases. The bound states of a vortex in $NbSe_2$ do not show the abrupt change when the magnetic field increases from 0.025 to 1.0 T [Fig. 3(b)]. The abrupt change should not be related to the proximity effect since it does not occur in the 2 QL Bi_2Te_3 film, as Fig. 3(c) shows. The dramatic change in the zero-bias peak intensity in 5 QL Bi_2Te_3 film is interpreted as the result of the coupling between adjacent vortices. At a small field, the distance between vortices is much larger than the vortex size, so the interaction between the vortices can be neglected. As the field increases to 0.18 T, the distance between two adjacent vortices is reduced to about 110 nm [Fig. 3(d)]. While the vortex size is around 35 nm, the interaction between the vortices becomes strong enough to destroy the Majorana modes. In this case, the LDOS at vortex cores is governed again by conventional quasiparticle bound states and a zero-distance splitting pattern recovers in the spatial variation of dI/dV spectra. This situation is shown in Fig. 3(e), which is in contrast to the finite-distance splitting at 0.1 T in Fig. 2(f).

We now discuss the difference in electronic structure of various quintuple layer systems. Figure 4 shows the evolution of the DOS near the Fermi level on Bi_2Te_3 films

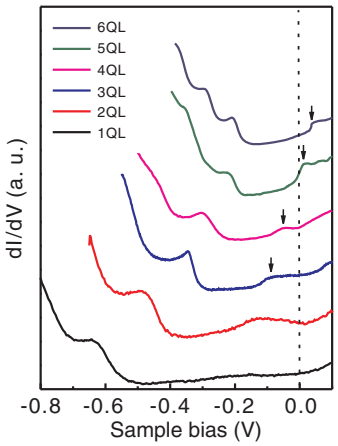

FIG. 4 (color). A series of dI/dV spectra measured on 1–6 QL Bi_2Te_3 films on $NbSe_2$ at 0.4 K. The curves become a deformed U-shape after the Dirac cone structure forms at 3 QL. The black arrows indicate the energy position of CBM, and the dashed line indicates the Fermi energy.

of various thicknesses obtained by STS. We can clearly see that TSS band or Dirac cone structure forms only when the thickness reaches 3 QL. Once the TSS band forms, the DOS curve exhibits a deformed U-shaped segment in the energy range between the bulk valence band maximum and conduction band minimum (CBM) [38,39]. In Fig. 4, arrows indicate the CBM, which shifts upward in energy as the thickness increases. It is seen that although the Dirac cone structure is formed at 3 QL, the Fermi level is about 100 meV higher than CBM, which means the bulk carrier density is still much higher than surface carrier density. So, the unconventional behavior from the TSS is submerged by that from bulk carriers. When the thickness reaches 4 QL, the Fermi level is almost at the CBM, and for 5 and 6 QL thin films, the Fermi level is a little bit lower than CBM. Therefore, the behavior related to TSS appears from 4 QL, and the Majorana mode can only be clearly observed on 5 or 6 QL films grown on $NbSe_2$.

Self-consistent evidence indicates that the Majorana mode exists in the vortex of the $Bi_2Te_3/NbSe_2$ heterostructure. Since the TSS is protected by the time reversal symmetry, the Majorana mode in our configuration is free from impurities and defects. It is also found that the Majorana mode can be tuned off by increasing the magnetic field. This might provide a route to controlling MFs for quantum computation.

The work was supported by the Ministry of Science and Technology (MOST) of China (2013CB921902, 2012CB927401, 2011CB921902, 2011CB922200, 2011CBA00108 and 2011CB922101), NSFC (91021002, 11174199, 11134008, 11274228, 11227404, 11023002, 11274269). F. C. Z. was partially supported by RGC GRF (707211).

J. P. X. and M. X. W. contributed equally to this work.

*Corresponding author.
canhualiu@sjtu.edu.cn
†Corresponding author.
jfjia@sjtu.edu.cn

[1] E. Majorana, Nuovo Cimento **14**, 171 (1937).
[2] F. Wilczek, Nat. Phys. **5**, 614 (2009).
[3] J. Alicea, Rep. Prog. Phys. **75**, 076501 (2012).
[4] C. W. J. Beenakker, Annu. Rev. Condens. Mater. Phys. **4**, 113 (2013).
[5] L. Fu and C. L. Kane, Phys. Rev. Lett. **100**, 096407 (2008).
[6] M. Z. Hasan and C. L. Kane, Rev. Mod. Phys. **82**, 3045 (2010).
[7] X.-L. Qi and S.-C. Zhang, Rev. Mod. Phys. **83**, 1057 (2011).
[8] A. C. Potter and P. A. Lee, Phys. Rev. B **83**, 184520 (2011).
[9] J. D. Sau, R. M. Lutchyn, S. Tewari, and S. Das Sarma, Phys. Rev. Lett. **104**, 040502 (2010); R. M. Lutchyn, J. D. Sau, and S. Das Sarma, Phys. Rev. Lett. **105**, 077001 (2010).
[10] V. Mourik, K. Zuo, S. M. Frolov, S. R. Plissard, E. P. A. M. Bakkers, and L. P. Kouwenhoven, Science **336**, 1003 (2012).
[11] M. T. Deng, C. L. Yu, G. Y. Huang, M. Larsson, P. Caroff, and H. Q. Xu, Nano Lett. **12**, 6414 (2012).
[12] A. Das, Y. Ronen, Y. Most, Y. Oreg, M. Heiblum, and H. Shtrikman, Nat. Phys. **8**, 887 (2012).
[13] A. D. K. Finck, D. J. Van Harlingen, P. K. Mohseni, K. Jung, and X. Li, Phys. Rev. Lett. **110**, 126406 (2013).
[14] E. J. H. Lee, X. Jiang, M. Houzet, R. Aguado, C. M. Lieber, and S. De Franceschi, Nat. Nanotechnol. **9**, 79 (2014).
[15] L. P. Rokhinson, X. Y. Liu, and J. K. Furdyna, Nat. Phys. **8**, 795 (2012).
[16] J. Liu, A. C. Potter, K. T. Law, and P. A. Lee, Phys. Rev. Lett. **109**, 267002 (2012).
[17] D. I. Pikulin, J. P. Dahlhaus, M. Wimmer, H. Schomerus, and C. W. J. Beenakker, New J. Phys. **14**, 125011 (2012).
[18] D. Bagrets and A. Altland, Phys. Rev. Lett. **109**, 227005 (2012).
[19] G. Kells, D. Meidan, and P. W. Brouwer, Phys. Rev. B **86**, 100503 (2012).
[20] S. Nadj-Perge, I. K. Drozdov, J. Li, H. Chen, S. Jeon, J. Seo, A. H. MacDonald, B. A. Bernevig, and A. Yazdani, Science **346**, 602 (2014).
[21] E. Dumitrescu, B. Roberts, S. Tewari, J. D. Sau, and S. Das Sarma, arXiv:1410.5412.
[22] F. Qu *et al.*, Sci. Rep. **2**, 339 (2012).
[23] P. Zareapour *et al.*, Nat. Commun. **3**, 1056 (2012).
[24] S. Cho, B. Dellabetta, A. Yang, J. Schneeloch, Z. Xu, T. Valla, G. Gu, M. J. Gilbert, and N. Mason, Nat. Commun. **4**, 1689 (2013).
[25] J. R. Williams, A. J. Bestwick, P. Gallagher, S. Sae Hong, Y. Cui, A. S. Bleich, J. G. Analytis, I. R. Fisher, and D. Goldhaber-Gordon, Phys. Rev. Lett. **109**, 056803 (2012).
[26] M.-X. Wang *et al.*, Science **336**, 52 (2012).
[27] J.-P. Xu *et al.*, Phys. Rev. Lett. **112**, 217001 (2014).
[28] C. Caroli, P. G. de Gennes, and J. Matricon, Phys. Lett. **9**, 307 (1964); R. G. Mints and A. L. Rakhmanov, Solid State Commun. **16**, 747 (1975).
[29] R. S. Akzyanov, A. V. Rozhkov, A. L. Rakhmanov, and F. Nori, Phys. Rev. B **89**, 085409 (2014).
[30] Y. E. Kraus, A. Auerbach, H. A. Fertig, and S. H. Simon, Phys. Rev. Lett. **101**, 267002 (2008).
[31] J. D. Sau, R. M. Lutchyn, S. Tewari, and S. Das Sarma, Phys. Rev. B **82**, 094522 (2010).
[32] C. K. Chiu, M. J. Gilbert, and T. L. Hughes, Phys. Rev. B **84**, 144507 (2011).
[33] Y. Y. Li *et al.*, Adv. Mater. **22**, 4002 (2010).
[34] G. Wang *et al.*, Adv. Mater. **23**, 2929 (2011).
[35] See Supplemental Material at http://link.aps.org/supplemental/10.1103/PhysRevLett.114.017001 for details of experiments and theoretical simulations.
[36] H. F. Hess, R. B. Robinson, R. C. Dynes, J. M. Valles, and J. V. Waszczak, Phys. Rev. Lett. **62**, 214 (1989).
[37] F. Gygi and M. Schlüter, Phys. Rev. B **43**, 7609 (1991).
[38] K. Park, J. J. Heremans, V. W. Scarola, and D. Minic, Phys. Rev. Lett. **105**, 186801 (2010).
[39] T. Zhang *et al.*, Phys. Rev. Lett. **103**, 266803 (2009).